

K. Grätz
M. Helmstedt
H.W. Meyer
K. Quitzsch

Structure and phase behaviour of the ternary system water, *n*-heptane and the nonionic surfactant Igepal® CA520

Received: 6 December 1996
Accepted: 2 September 1997

K. Grätz · K. Quitzsch
Institute of Theoretical
and Physical Chemistry
University of Leipzig
Linnéstr. 2, D-04103 Leipzig
Germany

M. Helmstedt (✉)
Institute of Experimental Physics I
University of Leipzig
Linnéstr. 5, D-04103 Leipzig
Germany

H.W. Meyer
Institute of Ultrastructure research
University of Jena
Ziegelmühlenweg 1, D-07743 Jena
Germany

Abstract The phase behavior of the system water, *n*-heptane and the nonionic surfactant Igepal® CA520 has been studied by visual inspection, high-performance liquid chromatography, polarizing microscopy and freeze-fracture electron microscopy. The phase diagram at 25 °C contains two large homogeneous microemulsion phases, an extended region of a lamellar liquid crystalline structure and some two- and three-phase regions. The oil-rich part of the phase diagram has been investigated by static and dynamic light scattering in order to examine the behavior of the collective

diffusion coefficient and the scattering intensity in the presence of increasing concentrations of water, starting from the binary system of *n*-heptane and Igepal® CA520. The results suggested that at a very low water content the aggregates of the microemulsion are small. With the exception of this region the structure is bicontinuous.

Key words Microemulsions – phase diagram – light scattering – microscopy

Introduction

Mixtures of the type water/oil/surfactant are applied in several industrial processes, e.g. in the oil industry in order to recover residual oil [1]. The phase behavior in ternary water/oil/nonionic surfactant mixtures has been studied by several authors [2–7]. The properties of such systems may be described in terms of these of the three binary subsystems, whereby the system oil/water is almost immiscible at normal temperatures, the system oil/nonionic surfactant usually is miscible at temperatures above the freezing point of water, and the aqueous solution of nonionic surfactant may contain besides a micellar solution several liquid crystal phases. This kind of system is characterized by the occurrence of an upper critical solu-

tion temperature called cloud point, at which temperature the aqueous surfactant solution splits up into a very dilute aqueous phase and a concentrated solution of the surfactant.

With certain mixtures of the three components a homogeneous transparent liquid phase of low viscosity and thermodynamical stability can be formed. Such systems are called microemulsions according to [8, 9]. Microemulsions exhibit their structure on a microscopic scale.

In this report we investigated the phase diagram of water/*n*-heptane/Igepal® CA520 at 25 °C and the phase behavior of the three components. Furthermore, we determined the collective diffusion coefficient in selected samples in order to study the microscopic structure in several microemulsions.

Experimental part

Chemicals

The nonionic surfactant Igepal® CA520 (C_8H_{17})– C_6H_4 – O – $(CH_2-CH_2-O)_5H$ (98%, Aldrich) and *n*-heptane (HPLC grade, Merck) were used without further purification. The water was doubly distilled.

Preparation of samples

Samples for phase-diagram studies were prepared by weighing and mixing the three components in glass ampoules which were flame-sealed and equilibrated at 25 °C. The samples for DLS studies were passed through a Sartorius Teflon filter with a pore diameter of 450 nm to remove all dust from them.

Phase diagram determination

The phase diagram has been determined by visual inspection, high-performance liquid chromatography, polarizing microscopy and freeze-fracture electron microscopy. The liquid crystalline phases were detected by a standard microscope (Zeiss, Germany) equipped with crossed polarizing filters. The freeze-fracture electron microscopy was performed with BAF 400 T (Balzers, Liechtenstein) and the electron microscopes EM 902A (Zeiss, Germany) and JEM 100B (Jeol, Japan). The fracture face of the samples was shadowed by Pt. Dynamic light scattering and PFG- 1H -NMR have been used to characterize the structures of microemulsion phases. Results of 1H -NMR self-diffusion measurements were published in [10]. The composition of the corresponding phases in equilibrium and the three-phase areas were determined by high-performance liquid chromatography (HPLC, Bischoff) with a Spherisorb ODS II column and a differential refractometer (Ri 8110, Bischoff) as detector. A spinning drop tensiometer SITE 04 (Krüss, Germany) was used to determine the interfacial tension of conjugate phases, while density was measured with a vibrating-tube densimeter DMA 60 (Paar, Austria).

Dynamic light scattering

From the intensity autocorrelation function, measured by dynamic light scattering (DLS),

$$G_2(t) = \langle I(0) I(t) \rangle \quad (1)$$

where $I(0)$ and $I(t)$ are the scattering intensity at the time 0 and t , resp., and $\langle \rangle$ is the time average, the field autocorrelation function $g_1(t)$ was determined according to the Siegert relation

$$G_2(t) = A + B g_1^2(t) \quad (2)$$

where A is the average uncorrelated scattering intensity and B an instrument parameter. For small monodisperse particles it is

$$g_1(t) = \exp(-Dq^2t) \quad (3)$$

Here $q = 4\pi n \sin(\Theta/2)/\lambda_0$ is the scattering vector, λ_0 is the wavelength of the incident light, n the refractive index of the medium, Θ the angle of observation, and t the time. $G_2(t)$ was measured with a DLS-SLS-5000 Laser Light Scattering Spectrometer/Goniometer (ALV, Langen, Germany) equipped with a diode-pumped, frequency-doubled Nd:YAG laser DPY 315II (Adlas, Lübeck, Germany, $\lambda_0 = 532$ nm) and a digital autocorrelator ALV 5000 at an observation angle of 90° and at $(25.00 \pm 0.01)^\circ C$. The intensity distribution was obtained by Laplace inversion of $g_1(t)$ by the program CONTIN [11].

From the measured count rate the integral scattering intensity was determined by calibration with benzene (absolute scattering intensity $I_v^{iso} = 12.86 \times 10^6 \text{ cm}^{-1}$ [12]), extrapolated for $\lambda = 532$ nm.

Results

Phase diagram

The ternary phase diagram of the system water/*n*-heptane/Igepal® CA520 at 25 °C is shown in Fig. 1. The concentrations are given in weight percent. The boundaries of various phases in the diagram have been located by visual inspection and HPLC.

The temperature of 25 °C is far above the cloud point for the aqueous solution of Igepal® CA520. For this reason we could not find a micellar phase in the water-rich part of the phase diagram, because in this temperature region the nonionic surfactant Igepal® CA520 is almost insoluble in water but can absorb water under formation of an isotropic solution phase up to 18 wt% water and a lamellar liquid crystalline phase between 18 wt% and about 70 wt% water.

The structure of the lamellar liquid crystalline phase has been characterized by polarizing microscopy and freeze-fracture electron microscopy. When microscopically observed between crossed polarization filters liquid crystalline samples show a characteristic mosaic texture. The texture of two samples is shown in Figs. 2A and B. The typical multilamellar structure of the liquid crystalline

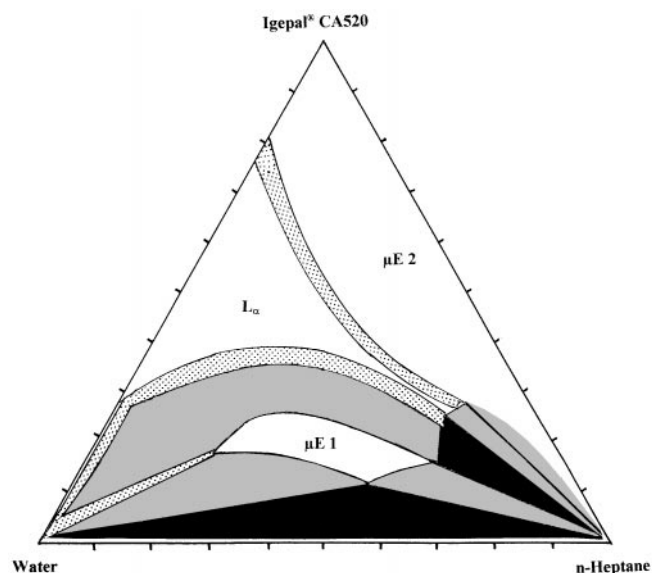


Fig. 1 Ternary phase diagram of water/*n*-heptane/Igepal® CA520 determined at 25 °C. Concentrations are given as percent per weight. One-phase regions are white, two-phase regions are grey, three-phase regions are black. Transition areas with undetermined structure are pointed. L_{α} : lamellar liquid crystal; μE 1: typical bicontinuous microemulsion; μE 2: W/O-microemulsion with several structures

phase has been visualized by freeze-fracture electron microscopy as shown in Fig. 3. Other mesomorphic phases like hexagonal or cubic liquid crystalline phases could not be observed. The phase diagram is dominated by a large one-phase region in the oil-rich part of the Gibbs triangle. Igepal® CA520 is almost completely miscible with *n*-heptane at 25 °C. The amount of water which can be solubilized by an Igepal® CA520/*n*-heptane mixture increases with increasing surfactant/oil ratio.

It is well established that several surfactants are able to form reverse micelles in apolar solvents, but that the association process is not comparable with the micellization process of surfactant molecules in aqueous solution. Mostly, the micellization process occurs neither with a sharply defined value of the critical micelle concentration (CMC) nor the associates are monodisperse in a narrow size distribution or with exactly determined geometrical shape.

The structure in that region was investigated by dynamic light scattering measurements and freeze-fracture electron microscopy. The results of the dynamic light scattering measurements will be given in more detail later. Two pictures made by freeze-fracture electron microscopy (Figs. 4A and B) show the structure of solutions with several concentrations of water with the same Igepal® CA520/*n*-heptane ratio of 1:1. In both of them it was not possible to distinguish the roughness of the surface caused

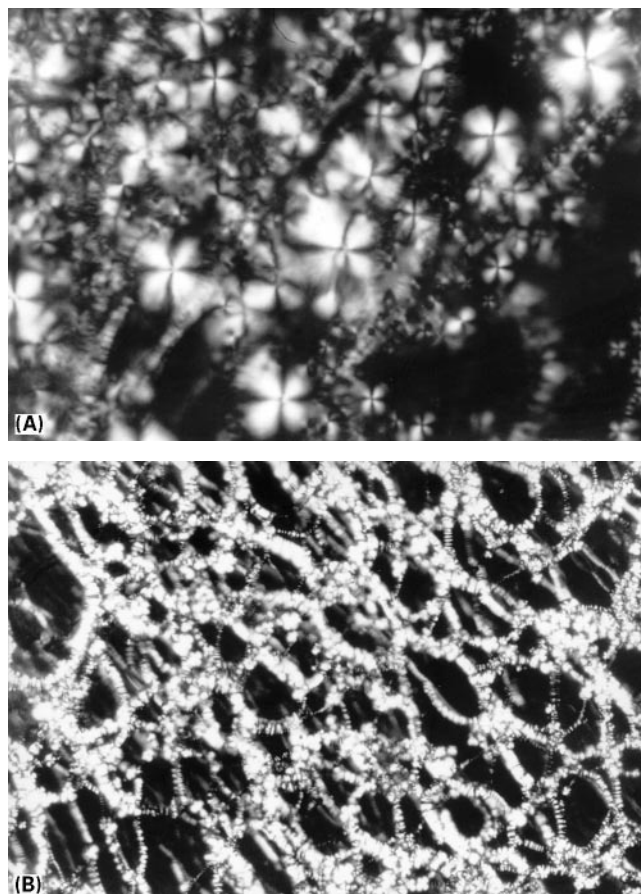


Fig. 2 Optical microscope patterns of samples between crossed polarizers: (A) characteristic mosaic texture of a lamellar liquid crystalline structure with 22 wt% water and 78 wt% Igepal® CA520. $\text{—} \triangle \text{—}$ 25 μm . (B) Network texture of the lamellar structure with 26 wt% water, 36 wt% *n*-heptane and 38 wt% Igepal® CA520. $\text{—} \triangle \text{—}$ 200 μm

by the experimental treatment from reversed micelles in the solution.

Another one-phase region occurs at about the same water and oil content and an Igepal® CA520 concentration between 12 and 30 wt%. The structure of this homogeneous isotropic solution has been studied by freeze-fracture electron microscopy, dynamic light scattering and ^1H -NMR self-diffusion measurements. Figure 5 shows the typical bicontinuous structure of the microemulsion as given in [13, 14].

At lower surfactant weight fractions the phase boundary divides the microemulsion phase from two two-phase regions and a large three-phase region. At a water/oil ratio of 1:1.5 and an Igepal® CA520 concentration below 15 wt% the system splits into three phases like a typical *Winsor III* system. Two of the phases are water and *n*-heptane both with quite low concentrations of surfactant. The third phase contains a higher amount of

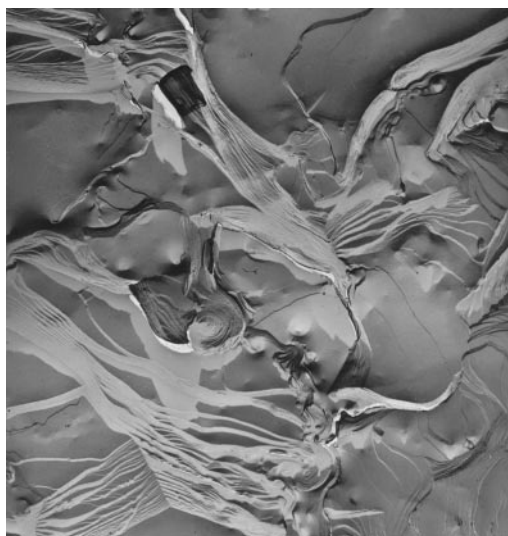


Fig. 3 Electron micrograph of the lamellar structure: composition 40 wt% water/60 wt% Igepal® CA520. $\longleftrightarrow \triangleq 2 \mu\text{m}$

surfactant and nearly the same weight percent of water and oil. The right side of the three-phase region is separated from a *Winsor I* system where the ternary system undergoes a liquid-liquid phase separation into an upper oil-rich and a lower surfactant-rich phase. On the left side of the three phase region there is a typical *Winsor II* system with a lower water phase and an upper solution with almost all of the surfactant. In all of the three *Winsor* systems the interfacial tension of conjugate phases was determined by means of the spinning drop method. The results of these measurements are reported in Table 1.

Dynamic light scattering

Examples for the measured intensity autocorrelation functions are given in Fig. 6. As expected, the translational diffusion coefficient decreases with increasing water content. Figure 7 shows the average scattering intensities as a function of the water content in mixtures with several Igepal® CA520/*n*-heptane ratios, which behave nonmonotonic. The scattering intensity first increases and reaches a maximum at a water content of about 2 wt%. Then the scattering intensity decreases with increasing weight percent of water until approximately 6 wt%. At a higher water content the values of the intensity are nearly constant.

The less the content of Igepal® CA520 in the mixture with *n*-heptane, the higher is the maximum of the scattering intensity. The corresponding behavior of the transla-

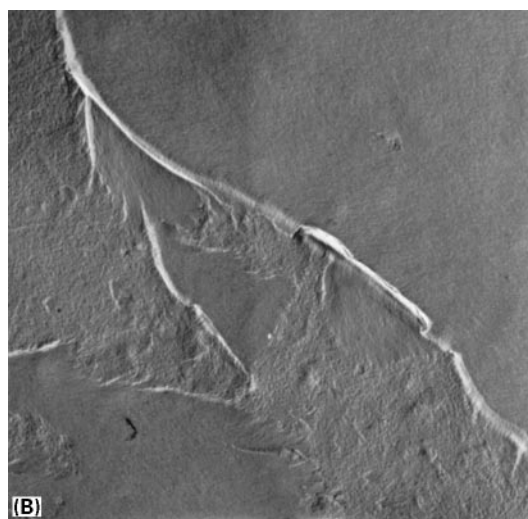
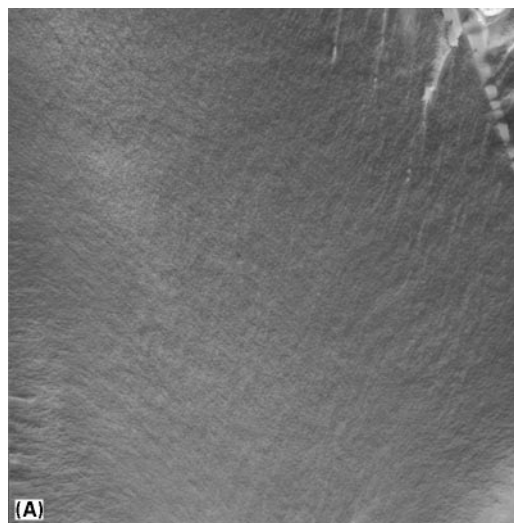


Fig. 4 Electron micrograph of the L_2 phase with a Igepal® CA520/*n*-heptane weight ratio of 1:1 and (A) 0.9 wt% water, $\longleftrightarrow \triangleq 1 \mu\text{m}$; (B) 5.7 wt% water, $\longleftrightarrow \triangleq 2 \mu\text{m}$

tional (mutual) diffusion coefficient $\langle D_t \rangle$ in dependence on the water content is shown in Fig. 8. The diffusion coefficients behave contrary to the scattering intensity. The diffusion coefficient first decreases and passes through a minimum at about the same water content as when the scattering intensity has reached the maximum. Then the amount of the diffusion coefficient slowly increases and becomes approximately constant at about 6 wt% water.

A dependence of the depth of the minimum on the quantitative composition of the binary Igepal® CA520/*n*-heptane mixture has not been found. The generally higher values of the diffusion coefficient at a mixture with at first

Table 1

Composition of the samples		Composition and density ρ of the corresponding phases			Interfacial tension [mN m ⁻¹]
		Upper (1)	Middle (2)	Lower (3)	
Water	48 wt%		36 wt%	≈ 100 wt%	(1)/(2) 0.004
<i>n</i> -heptane	49 wt%	99 wt%	52 wt%		
Igepal® CA520	3 wt%	1 wt%	12 wt%		(2)/(3) 0.002
ρ [g cm ⁻³]		0.6803	0.8746	0.9974	
water	60 wt%	37 wt%		≈ 100 wt%	(1)/(3) 0.016
<i>n</i> -heptane	28 wt%	13 wt%			
Igepal® CA520	12 wt%	50 wt%			
ρ [g cm ⁻³]		0.8272		1.0110	
water	14 wt%			33 wt%	(1)/(3) 0.019
<i>n</i> -heptane	80 wt%	98 wt%		54 wt%	
Igepal® CA520	6 wt%	2 wt%		13 wt%	
ρ [g cm ⁻³]		0.6724		0.9135	

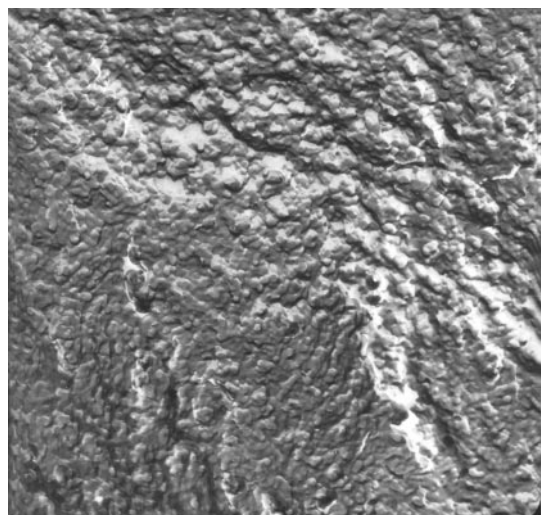


Fig. 5 Electron micrograph of the bicontinuous structure of a micro-emulsion system with 40 wt% water, 40 wt% *n*-heptane and 20 wt% Igepal® CA520; $\overline{\quad\quad\quad} \triangleq 1 \mu\text{m}$

70 wt% Igepal® CA520 and 30 wt% *n*-heptane are so because of the higher viscosity of these mixtures.

Discussion and conclusions

We investigated the ternary system water, Igepal® CA520 and *n*-heptane by a number of experimental approaches as phase equilibria determination by visual inspection and high-performance liquid chromatography, phase characterization by polarizing, freeze-fracture electron micro-

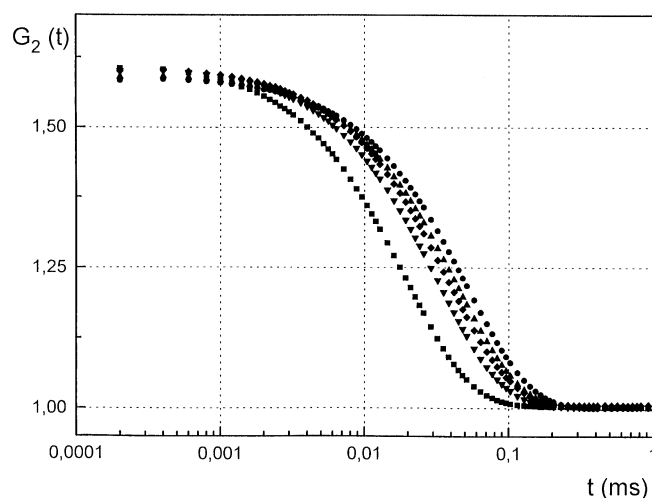


Fig. 6 Intensity autocorrelation functions $G_2(t)$ ■ of mixtures of 40 wt% Igepal® CA520 and 60 wt% *n*-heptane, ▼ 0.46 wt%, ◆ 0.82 wt%, ▲ 1.03 wt% and ● 1.52 wt% water that were added to the amount of the binary mixture, which was set to 100%

scopy and measurements of the interfacial tension by spinning drop tensiometry. The study also provides interesting information on the intrinsic structure of micro-emulsion phases mainly determined by dynamic light scattering and several microscopic techniques.

The phase diagram is dominated by a large liquid crystalline lamellar phase, an extensive isotropic homogeneous solution in the oil-rich part of the diagram and a three phase region at lower surfactant concentrations. The formation of the lamellar liquid crystalline phase in the binary system water/Igepal® CA520 can be explained

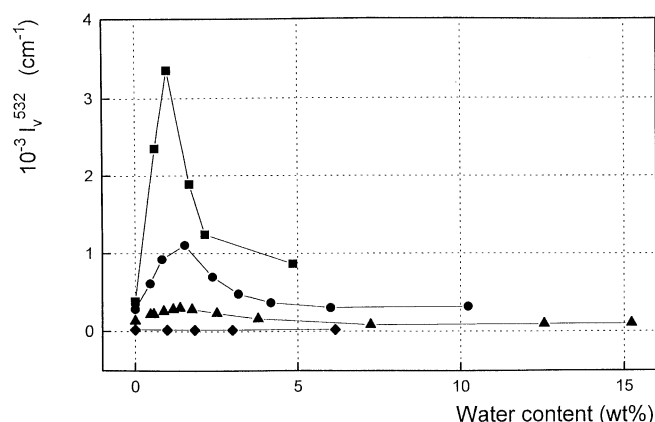


Fig. 7 Scattering intensity I_{90} vs. the water content in mixtures of Igepal® CA520/*n*-heptane with ■ 30 wt%, ● 40 wt%, ▲ 50 wt% and ◆ 70 wt% Igepal® CA520. Water was added to the binary mixtures (according to Fig. 6 legend)

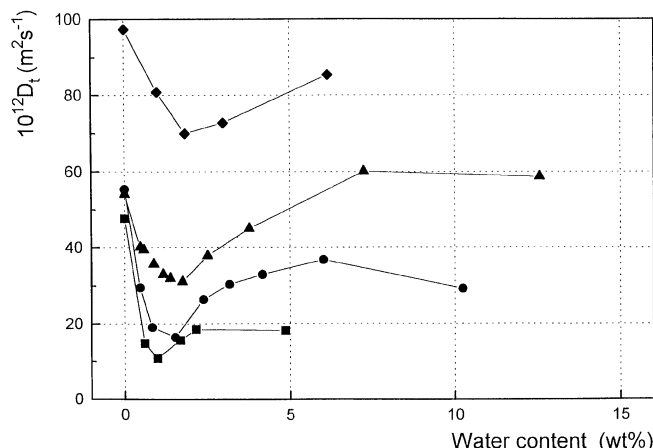


Fig. 8 Translational diffusion coefficient D_t vs. the water content in mixtures of Igepal® CA520/*n*-heptane with ■ 30 wt%, ● 40 wt%, ▲ 50 wt% and ◆ 70 wt% Igepal® CA520. Water was added to the binary mixtures (as described by Fig. 6)

by means of the theory by Heusch [15]. He investigated the influence of water on the structures of aqueous solutions of surfactants. In aqueous solution of nonionic surfactants such as polyglycoethers the water molecules are attached to the oxygen atoms of the oxyethylene chains of surfactant molecules. If at least one water molecule is bound by each of the oxyethylene groups, hydrogen bridge linkages between the surfactant molecules lead to the formation of layers. Such layers are the units which form liquid crystalline structures. At a composition of 18 wt% water and 72 wt% Igepal® CA520 the ratio of the water molecules to the surfactant molecules is 5:1, that is about each of the oxyethylene group of the Igepal® CA520 molecule is attached to one water molecule and the formation of the lamellar liquid crystalline structure begins. The clear characterization of this structure was verified by the comparison of the polarizing microscopic texture of the samples with the system of Ekwall [16]. Because of the strong hydrophobicity of the surfactant we could not find an aqueous micellar solution in the water-rich corner of the phase diagram. The cloud point is well below 5 °C, and owing to this fact hexagonal liquid crystalline phases are not observable in the phase diagram. Apparently, there is a small region with a different structure expanding next to the concentration region of lamellar structure. The samples in this region have a significantly higher viscosity than other samples. Unfortunately, a typical texture was not observable.

With some simplifications we have applied the theory of Heusch to the ternary system water/Igepal® CA520/*n*-heptane in order to explain the results of scattering measurements in the microemulsion region. The behavior

of the diffusion coefficient and the scattering intensity in dependence on the water content (Figs. 7 and 8) indicate that there is a structural transition at a water content of about 2 wt%. Several studies of the aggregate structure in reversed micellar solutions by dynamic light scattering have been published recently [17–22]. The results of dynamic light scattering measurements in fairly dilute systems indicate clearly the formation of very small, spherical aggregates. Figures 7 and 8 suggest that the aggregate size increases with increasing content of water till about 2 wt% at a constant ratio of *n*-heptane and Igepal® CA520. At this water content the ratio of the water molecules to the surfactant molecules is 1:1.3. Probably there are only few surfactant molecules attached to one or two water molecules to form aggregates similar to reverse micelles. At higher water content, a decrease of the scattering intensity and an increase of the mutual diffusion coefficient can be observed. This behavior indicates that the small aggregates break down. Now the surfactant molecules must be rather monodisperse in the *n*-heptane solution attached by some water molecules. With increasing water content the interaction between the water molecules leads to the formation of a bicontinuous microemulsion structure. At a water content of about 10 wt% the scattering intensity and the diffusion coefficient become nearly constant at higher concentrations of water. This behavior clearly shows that the microemulsion structure does not change.

Acknowledgements The authors wish to thank Dr. K. Kirmse for the determination of the interfacial tension. This work has been supported by the Deutsche Forschungsgemeinschaft (Graduiertenkolleg "Physikalische Chemie der Grenzflächen" and SFB 294).

References

1. Healy RN, Reed RL (1977) Soc Pet Eng J 129
2. Kahlweit M, Leßner E, Strey R (1983) Colloid Polym Sci 261:954
3. Kahlweit M, Strey R, Haase D, Firman P (1988) Langmuir 4:785
4. Kahlweit M, Strey R, Busse G (1990) J Phys Chem 94:3881
5. Shinoda K, Kunieda H (1973) Colloid Interface Sci 42:381
6. Shinoda K, Ogawa T (1967) Colloid Interface Sci 24:56
7. Friberg S, Buraszczenka I (1987) Prog Colloid Polym Sci 63:10
8. Hoar TP, Schulman JH (1943) Nature 152:102
9. Schulman JH, Stoeckenius W, Prince LM (1959) J Phys Chem 63:1677
10. Fleischer G, Grätz K, Kärger J, Meyer HW, Quitzs K (1997) J Colloid Interface Sci 190:9
11. Provencher SW (1982) Computer Phys Commun 27:213, 229
12. Millaud B, Strazielle C (1979) Makromol Chem 180:441
13. Jahn W, Strey R (1988) J Phys Chem 92:2294
14. Vinson PK, Sheehan JG, Miller WG, Scriven LE, Davis HT (1991) J Phys Chem 95:2550
15. Heusch R (1991) Tenside Surf Det 28:38
16. Ekwall P (1975) Advances in Liquid Crystals, Vol 1. Academic Press, New York
17. Sjöblom J, Rosenqvist K, Stenius P (1982) Colloid Polymer Sci 260:82
18. Svård M, Schurtenberger P, Fontell K, Jönsson B, Lindman B (1988) J Phys Chem 92:2261
19. Schurtenberger P, Peng Q, Leser ME, Luisi P-L (1993) J Colloid Interface Sci 156:43
20. Tricot Y, Kiwi J, Niederberger W, Grätzel M (1981) 85:862
21. D'Aprano A, D'Arrigo G, Paparelli A, Goffredi M, Liveri VT (1993) J Phys Chem 97:3614
22. Cazabat AM, Langevin D (1981) J Chem Phys 74:3148